A Comparison of Estimates of Atmospheric Effects on Signal Propagation Using ITU Models: Initial Study Results

David D. Morabito*

ABSTRACT. — This article provides details on a comparison performed on calculated atmospheric effects on signal propagation using different methods for the Deep Space Network (DSN) and two Near Earth Network (NEN) sites commonly used in telecommunications link budgets. Atmospheric attenuation and scintillation fading are two of the many contributors that need to be taken into account in such link budgets between transmitter and receiver. Although atmospheric noise temperature increase is another contributor (at the receiver), it is well related to atmospheric attenuation through appropriate model equations. Telecommunication engineers working NEN link budgets make use of data and models obtained from the International Telecommunication Union (ITU) in order to estimate atmospheric effects. Such effects include atmospheric attenuation (gaseous, rain, and cloud), atmospheric noise temperature contribution, and scintillation. Because most NEN links usually operate at very high margins, uncertainties in the ITU models were not much of a concern in the past as they tended to be conservative, in comparison to links of the DSN that operate at low margins and thus require more accurate statistics on atmospheric effects. Such statistics for the DSN links make use of brightness temperature measurements from multiyear water vapor radiometer (WVR) data from instruments operating at the DSN sites. Atmospheric attenuation statistics derived from WVR data are well documented and are published by the DSN. Thus, the DSN sites make a good testbed in which to cross-compare atmospheric loss statistics with those derived from ITU data and models.

I. Introduction

This article compares the atmospheric losses derived from different methods for the Deep Space Network (DSN) and some Near Earth Network (NEN) sites for use in telecommunications link budgets. Although atmospheric noise temperature increase is another contributor (at the receiver), it is well related to atmospheric attenuation through appropriate modeling and, thus, this article will focus on atmospheric attenuation and scintillation fading.

* Communications Architectures and Research Section.

The research described in this publication was carried out by the Jet Propulsion Laboratory, California Institute of Technology, under a contract with the National Aeronautics and Space Administration. © 2014 California Institute of Technology. U.S. Government sponsorship acknowledged.

The NEN makes use of data and models of the International Telecommunication Union (ITU) in order to estimate atmospheric effects in their telecommunications link budgets. Such effects include atmospheric attenuation (gaseous, cloud liquid, and rain), atmospheric noise temperature contribution, and scintillation. Other effects covered in ITU models such as rain depolarization will not be addressed in this article. Since most NEN links usually operate at high margins, uncertainties in the ITU models were not as much of a concern, versus uncertainties in DSN links, which operate at very low margins and thus require more accurate statistics on atmospheric effects. Atmospheric degradation statistics for the DSN are obtained from brightness temperature measurements at 31.4 GHz from multiyear data sets from water vapor radiometers (WVRs) operating at the DSN sites. Since the DSN accounts for atmospheric attenuation estimated from WVR brightness temperature measurements as published in the *DSN Telecommunications Link Design Handbook* [1], atmospheric loss statistics for these sites make a good testbed in which to conduct cross-comparisons with those estimated from ITU data and ITU models. In addition, with higher data rates being considered for future near-Earth missions, the results of this study will provide a benchmark on the accuracy of using ITU models and data for lower margin link scenarios.

All of the DSN WVRs are multifrequency instruments, even though we only make use of the 31.4-GHz channel brightness temperatures to estimate the attenuation statistics used in this article. It is intended to extract water vapor content and liquid content statistics from the multifrequency WVR data sets for a future follow-on study. Such meteorological parameters will then be compared to those obtained from ITU global maps such as of integrated water vapor as well as performing similar comparisons by feeding these into the ITU-R prediction methods.

This article presents a comparison of total attenuation (including gaseous, cloud liquid, and rain contributors) between different ITU models and their inputs. Inputs to the ITU models that estimate this quantity include surface water vapor density, cloud liquid, and rain rate for given cumulative distribution values, rain height, and nominal values of the dry atmosphere (pressure and air temperature) for a given site. Surface water vapor density, rain rate, median wet refractivity (for scintillation), and cloud liquid statistics have been extracted from ITU global maps of these quantities as well as calculated from multiyear surface weather data sets near the selected sites used for the comparison. Interpolation procedures have been applied to the ITU global maps of the various quantities to refer them to the longitude and latitude of the site of interest.

II. ITU Models

A. Meteorological Parameters

According to ITU-R P.453-10 [2], the wet term of the radio refractivity is given by

$$N_{wet} = 3.732 \times 10^5 e/T^2 \tag{1}$$

where e is water vapor pressure in hPa (or mbar), and T is absolute temperature in K. This quantity is used as one of the inputs to the ITU scintillation model and does not directly appear in the calculations for gaseous, cloud, and rain attenuation.

Gaseous attenuation is derived from ITU models with water vapor pressure as the principal input, which requires meteorological surface data inputs of relative humidity RH (in percent) and saturated water vapor pressure e_s (in hPa):

$$e = RH\, e_s / 100 \tag{2}$$

The saturated water vapor pressure e_s (in hPa) is a function of surface pressure and surface temperature where a series of coefficients are utilized for both water and ice (ITU-R P.453-10 [2]).

Finally, surface water vapor density ρ (g/m^3) can be estimated from water vapor pressure as follows:

$$\rho = \frac{216.7e}{T} \tag{3}$$

where T is air temperature (in K). Surface water vapor density is the prime input to the ITU models that calculate atmospheric gaseous attenuation. In addition to surface water vapor density, the ITU models that are used to calculate gaseous atmospheric attenuation also require station height above sea level (km), frequency (GHz), atmospheric pressure at the station location p (hPa), mean temperature at the station location t deg C), and elevation angle, θ. From these, the following parameters are calculated: h_0, the equivalent oxygen height at the Earth station site in km; γ_0, the specific attenuation at ground level due to dry air (dB/km); h_w, the equivalent water vapor height at the Earth station site (km); and γ_w, the specific attenuation at ground level due to water vapor (dB/km) [3]. The station height above mean sea level values that were used in the model were 0.991 km for Goldstone, 0.765 km for Madrid, and 0.673 km for Canberra.[1] It is believed that these values lie close to the height of the WVR locations whose data were used in the comparisons.

The zenith attenuation in dB due to both dry air and water vapor is then calculated as [3]

$$A = h_0\gamma_0 + h_w\gamma_w\,. \tag{4}$$

The attenuation through the atmospheric ray path of the signal, B, in dB, at a given elevation angle θ (for $\theta > 10$ deg) is given by [3]

$$B = \frac{A}{\sin(\theta)}. \tag{5}$$

One method to obtain surface water vapor density statistics and median refractivity values used as input to the ITU models is to use global ITU maps (ITU-R P.453-10 [2]) where the longitude and latitude of the site are inputs to a look-up of this quantity. Another method is to estimate these quantities from surface meteorological data acquired from weather stations residing near or within the tracking sites (ITU-R P.453-10 [2], ITU-R P.836-3 [4]). The resulting outputs are then taken to be representative of the site.

[1] S. Slobin, personal communication, Jet Propulsion Laboratory, Pasadena, California, August 2014.

The various ITU meteorological maps are on a 1.125-deg by 1.125-deg grid. Depending on the latitude, the value at a given grid point represents an average over an approximately 100-km by 100-km area. As a result, the maps are an approximation to the macroclimate and do not predict the detailed microclimate. For example, the rainfall rate map will predict the rainfall rate distributions for Redondo Beach, Malibu, and Pasadena in California to be very similar; however, due to the microclimates and orography, the actual rainfall rate distributions will be significantly different. The ITU-R recommendations recognize that the digital maps are macro estimates.[2] According to ITU-R P.618 [15], the next most accurate method involves obtaining long-term rain statistics from surface meteorological instruments residing next to or near the tracking station of interest. Thus, if this long-term statistic cannot be obtained from local data sources, an estimate can be obtained from the maps of rainfall rate provided given in Recommendation ITU R P.837 [9]. Since such data only include values of meteorological quantities taken near the surface, they are not representative of atmospheric effects occurring higher up in altitude. However, the models assume certain dependencies of these parameters with altitude. The next most accurate method would involve making use of integrated water vapor and liquid content statistics to extract attenuation statistics. However, such comparisons involving these data types are focus for future study and are outside the scope of this article.

As previously discussed, estimating the given quantities from such measurements taken near or at the station should be more accurate than those obtained from ITU global maps. The DSN sites have operating weather stations residing near their antennas from which to derive quantities such as surface water vapor density and refractivity. In addition, some of the NEN sites have weather stations operating within the complexes such as at White Sands, New Mexico [5] and Svalbard, Norway [6]. Thus, multiyear weather data sets from these complexes were constructed and analyzed. Consequently, wet refractivity and surface water vapor density values were estimated from the surface weather measurements using standard ITU models. The statistics of these quantities were then extracted for use in ITU worksheet tools that estimate the various quantities for 50 percent, 90 percent, 95 percent, 99 percent, and (in some cases) 99.9 percent availabilities and as a function of link frequency and elevation angle.

In all cases where ITU global maps were used, the parameters of interest were extracted using a look-up procedure that used the longitude and latitude of the site to extract the four grid points that were nearest to the site. A bilinear interpolation of the four grid points as described in Annex 1 of ITU-R P.1144-6 [23] was then performed. Most cases involved a grid spacing of 1.125 deg by 1.125 deg. ITU values of rain height were obtained from maps with a grid spacing of 1.5 deg by 1.5 deg.

B. Rain Attenuation

There is a well-developed theory relating signal attenuation along an Earth–space path to the point rainfall rate at the Earth station [7]. Rain attenuation is estimated in ITU models

[2] H. Berger, personal communication, Northrop Grumman Corporation, November 2014.

using the specific attenuation due to rain γ_R (in dB/km), which is obtained from the rain rate R (mm/h) that is exceeded 0.01 percent of a year for a particular site via the following formulation (ITU-R P.838-3 [8]):

$$\gamma_R = k\, R^{\alpha} \tag{6}$$

where k and α are functions of frequency and coefficients for horizontal or vertical polarization, and are obtained from ITU table look-up. The ITU-R P.838-3 [8] document also provides formulas for α and k for the case of circular polarization (the case of interest here), which also includes a function of path elevation angle and polarization tilt angle. The rain rate R for p = 0.01 percent is obtained using the procedure outlined in ITR-R P.837-5, Annex 1 [9–11]. This procedure takes as input the probability level (set to p = 0.01 percent) and the latitude and longitude of the ground site, and then outputs the rainfall rate for a given probability (see below).

In addition, the rain attenuation model calculations also require a rain height h_R (in km) above sea level for the site obtained from ITU-R P.839-3 [12]. This is defined as the height to which rain extends during precipitation periods.[3] The rain height can be estimated (ITU-R P.839-3 [12]) via the following:

$$h_R = h_0 + 0.36 \text{ km} \tag{7}$$

where h_0 is the mean 0 deg C isotherm height above mean sea level that can be obtained from a global map of this quantity (ITU-R P.839-3 [12]). The rain rate is obtained via look-up of an electronic "global map" file of this quantity using the latitude and longitude of the ground site as input and applying the bilinear interpolation.

Other steps used to calculate rain attenuation are documented in ITU-R SA.2183 [3] that provides for calculation of slant path, effective path length (L_e), and attenuation for 0.01 percent of a year, $A_{0.01}$:

$$A_{0.01} = \gamma_R L_e. \tag{8}$$

The effective path length (L_e) is based on the actual propagation path between the Earth station and the rain height as modified by vertical reduction and horizontal adjustment factors that account for the rainfall distribution along the propagation path.

From $A_{0.01}$, the rain attenuation for any exceedance probability p is estimated using ITU-R SA.2183 [3]:

$$A_p = A_{0.01}\left(\frac{p}{0.01}\right)^{-\left(0.655+0.033\ln(p)-0.045\ln(A_{0.01})-\beta(1-p)\sin\theta\right)} \tag{9}$$

where β is a function of station latitude, elevation angle, and exceedance probability, and θ is station elevation angle.

[3] The height of the 0 deg C isotherm is sometimes referred to as the "bright band," so named because radar echoes were observed at this height due to coalescence and melting of snowflakes, the result of a well-defined "melting" layer that reflects the radar signals.

In this article, rain attenuation is predicted using the ITU-R rain attenuation prediction method, where the rainfall rate is determined: a) from the ITU-R maps, and b) from an alternate method developed by S. Slobin based on total rainfall measurements taken near the DSN sites.

C. Gaseous Attenuation

Gaseous attenuation is computed in the form of attenuation coefficients in dB/km for both dry air γ_0 and water vapor γ_w using equations provided in Annex 2 of ITU-R P.676.9 [13]. The dry-air coefficient is evaluated from mean values of surface pressure and air temperature. Annual mean surface air temperature can be obtained from maps given in ITU-R P.1510 [14]. These components do not vary significantly and it is assumed that mean values of temperature and pressure are sufficient for use in the models. The water vapor coefficient depends on surface water vapor density, which can be obtained from ITU global maps or from surface weather data. This article discusses a direct comparison between attenuation calculated from surface water vapor density obtained from global ITU maps and from surface water vapor density obtained from several years of recent surface weather data for the three DSN sites and two selected NEN sites using the ITU model formulas described in this section.

The attenuation coefficients can then be referred to the slant path of interest (along a given elevation angle) for a site at a specified altitude, making use of equivalent heights for both dry air and water vapor (ITU-R P676-9 [13]).

In this article, gaseous attenuation is predicted using the ITU-R gaseous attenuation prediction method, where the surface water vapor density is determined: a) from the ITU-R maps, and b) from local measured data.

D. Attenuation due to Clouds and Fog

The contribution of attenuation due to cloud liquid was determined using the procedure outlined in ITU-R P.840-6 [22] using

$$A = \frac{L_{red} K_l}{\sin\theta}$$

where L_{red} is the total columnar content of liquid water reduced to a temperature of 0 deg C (in kg/m^2 or mm), K_l is the specific attenuation coefficient at the frequency of interest, and θ is the elevation angle. The values of L_{red} were obtained using bilinear interpolation of annual maps of this quantity of grid-spacing resolution 1.125 deg by 1.125 deg in longitude and latitude using the site coordinates as input. The maps were available for the different values of probability exceedance.

In this article, cloud attenuation is predicted using the ITU-R cloud attenuation prediction method and cloud liquid water from the ITU-R maps.

E. Scintillation

Scintillation fading or loss was estimated as outlined in Section 2.4.1 of ITU-R P.618-10 [15]. The principal input was wet refractivity, N_{wet}. This quantity was obtained from surface maps provided in ITU-R P.453 [2] for one method. In the other method, surface weather data were used to compute N_{wet} and its statistics from several years of surface temperature and relative humidity measurements using formulation provided in ITU-R P.453 [2] and as summarized in Section II.A. This scintillation fading model (Karasawa model) is applicable for elevation angles above 4 deg. Since most cases of tracking spacecraft involve higher elevation angles, this model is sufficient for estimating scintillation fading. The ITU also has a deep fading model that covers very low elevation angles ~0 deg to ~1 deg [15]. Lee, Cheung, and Ho, 2011 [16] present a unified scintillation model approach that provides continuity between the very low deep model starting near 1-deg elevation and the higher elevation Karasawa model starting near 5-deg elevation. This unified scintillation model has since been adopted by the ITU. For this article, we are only concerned with elevation angles >10 deg, and thus the Karasawa model suffices.

F. Total Loss Using ITU Models

Once attenuation and other atmospheric quantities are estimated from these methods, they can be compared. The overall attenuation is calculated per ITU methodology as (ITU-R P.618-11 [15]):

$$A_T(p) = A_G(p) + \sqrt{\left(A_R(p) + A_C(p)\right)^2 + A_S^2(p)}. \tag{10}$$

In cases where total attenuation is compared to that extracted from DSN WVR brightness temperature measurements, the contribution of scintillation is neglected since the WVR measurements are not sensitive to this nonthermal contribution. In this case, this equation thus reduces to

$$A_T(p) = A_G(p) + A_R(p) + A_C(p). \tag{11}$$

Equation (11) is valid for p equal to or greater than 1 percent. However, ITU-R P.618-11 [15] states that a large part of the cloud attenuation and gaseous attenuation is already included in the rain attenuation prediction for time percentages below 1 percent. Thus, for p <1 percent, $A_G(p) = A_G(1\%)$ and $A_C(p) = A_C(1\%)$ in Equation (11).

Total atmospheric attenuation A_T simplifies to the direct sum of gaseous (A_G), rain (A_R), and cloud (A_C) attenuation if we assume scintillation fading is negligible or not applicable.

Other ITU documents that were used in the course of this study are references [17–19].

III. Meteorological Parameter Statistics Derived from ITU Global Maps and Weather Data

Table 1 provides estimates of median refractivity (used to calculate scintillation fading) for each of the three DSN sites — Goldstone, Madrid, and Canberra — as well as the two

Table 1. Wet refractivity statistics.

Site Location	Median Refractivity Global Maps, N units	Median Refractivity Weather Data, N units	Number of Weather Records	Span of Weather Data
Goldstone	20.925	24.816	2,151,999	2009–2013
Madrid	33.799	38.705	2,497,597	2009–2013
Canberra	40.461	43.655	3,010,376	2008–2013
White Sands	24.378	20.923	2,437,900	2009–2013
Svalbard	14.075	18.782	1,246,902	2011–2013

NEN sites, White Sands and Svalbard. The third column provides estimate of the median refractivity calculated from weather data for recent years where the number of weather data records shown in the fourth column covers the span of data in years shown in the fifth column of Table 1. For comparison, the value for median refractivity of the site obtained from ITU global maps is shown in the second column.

Table 2 displays the values of surface water vapor density at given probabilities for each of the DSN sites extracted from ITU global maps of these quantities and from direct calculation from several years of recent surface weather data acquired at each of these sites (see Table 1). Table 3 provides the same information for the two NEN sites in this study, White Sands and Svalbard.

Table 2. Surface water vapor density statistics, DSN sites.

	Goldstone		Madrid		Canberra	
	Weather Data	ITU Global Maps	Weather Data	ITU Global Maps	Weather Data	ITU Global Maps
p	Vapor Density, g/m^3	Vapor Density, g/m^3	Vapor Density, g/m^3	Vapor Density, g/m^3	Vapor Density, g/m^3	Vapor Density, g/m^3
0.5	4.13	5.00	6.45	6.55	7.38	7.39
0.9	7.19	7.87	9.40	9.32	12.13	11.39
0.95	8.56	8.85	10.24	10.12	13.39	12.52
0.99	12.34	11.49	12.02	11.58	15.80	14.59
0.999	15.38	15.97	13.60	13.03	18.01	16.81

Table 3. Surface water vapor density statistics, selected NEN sites.

	White Sands		Svalbard	
	Weather Data	ITU Global Maps	Weather Data	ITU Global Maps
p	Vapor Density, g/m^3	Vapor Density, g/m^3	Vapor Density, g/m^3	Vapor Density, g/m^3
0.5	3.38	4.52	2.87	2.65
0.9	9.40	10.46	5.51	5.02
0.95	11.08	12.36	6.14	5.44
0.99	13.60	14.61	7.19	6.14
0.999	15.28	16.09	8.14	6.78

Figure 1 displays the cumulative distribution (CD) of the surface water vapor density estimates (solid curves) calculated from local weather data at the three DSN sites as well as for two NEN sites, White Sands and Svalbard. Also shown in Figure 1 are the global ITU map values (dashed curves). Note that the best agreement is achieved for Madrid where the global map curve lies almost on top of the weather data curve. There is reasonable agreement for Svalbard and Canberra between the two curves. The Goldstone weather data curve lies to the left of the ITU map curve, perhaps suggesting that the recent years of weather were drier for the California desert environment compared to the 30-plus years on which the global map values were based. The two White Sands curves have somewhat gentler downward slopes than those for the other sites with the weather data curve again lying to the left of the ITU global map curve, again suggesting that the recent few-year weather data set was indicative of drier conditions in the American Southwest. Of the three DSN sites, Goldstone has the lowest surface water vapor density for a given CD and Canberra has the highest.

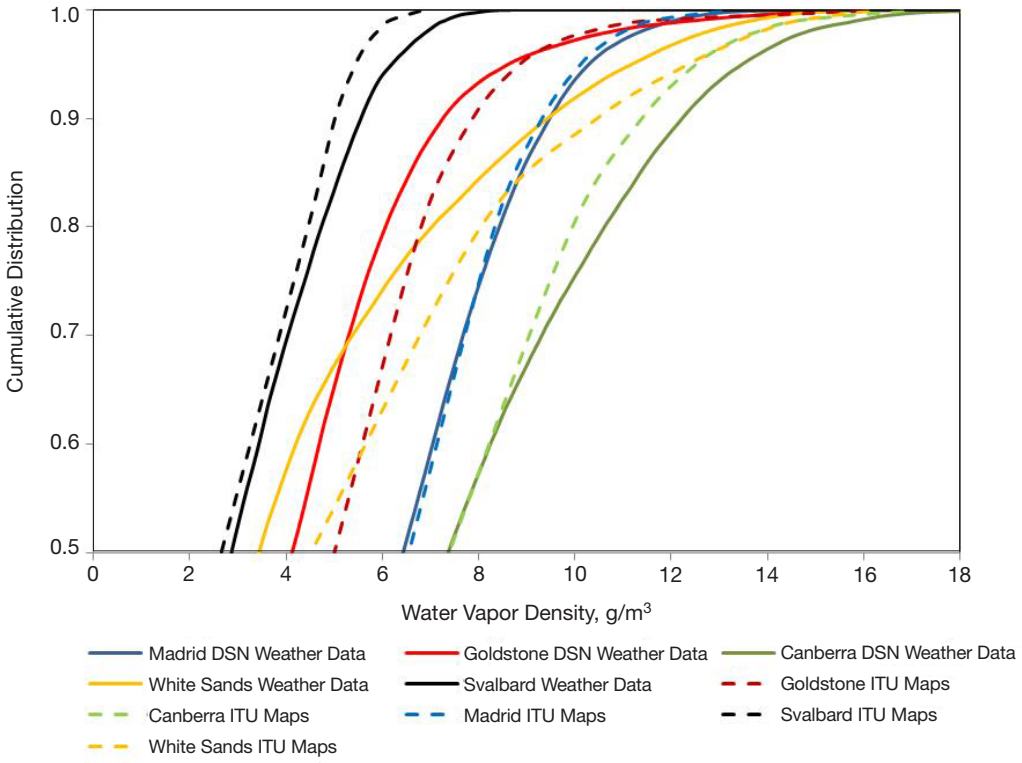

Figure 1. Cumulative distribution of surface water vapor density for different sites extracted from several years of weather data (solid curves) and ITU global map values (dashed curves).

Table 4 displays the rainfall rates and rain heights obtained from ITU global maps using the documented procedures [9–12] (Section II.B) for the sites discussed in this article. Also presented in Table 4 are alternative 0.01 percent rain rates ($R_{0.01}$). The alternative Goldstone, Canberra, and Madrid rain rates in Table 4 were obtained from S. Slobin[4] using a technique that calculates these from yearly average rainfall totals from the DSN sites (and other

[4] S. Slobin, personal communication, Jet Propulsion Laboratory, Pasadena, California, August 2014.

Table 4. ITU rain parameters.

Site	ITU Global Map 0.01% Rain Rate, mm/h	ITU Global Map Rain Height, km	Alternative 0.01% Rain Rate, mm/h	Source of Alternative Rain Rates
Goldstone	18.8183	2.923	5.75	Slobin 2014
Canberra	41.736	3.689	38.18/13.00	Slobin 2014/fit to data
Madrid	29.1385	2.939	16.07	Slobin 2014
White Sands	35.502	4.744	—	—
Svalbard	12.540	1.913	—	—

nearby weather stations) from the *DSN Telecommunications Link Design Handbook* (DSN 810-005) [1]. The span of the rain data used for each site is as follows: Goldstone (1973–2000), Canberra (1966–2002), and Madrid (1961–1990) [1]. This technique makes use of the Crane rain rate distribution curves (percent of time particular rain rates are exceeded) [20], scaling the rain rates appropriately such that the resulting average rainfall total matches that provided in [1], but retaining the shape of the curves. For example, the curve for the entire southwest United States [20] gives a factor of four too much rain for the Goldstone desert climate, and thus this adjustment is expected to provide a more reasonable estimate of the actual rain rate statistics.

The Slobin rain rate for Canberra (38.18 mm/h) was close in value to the ITU Global Map value (41.736 mm/h), which produced values of attenuation that were close to each other but very high relative to the DSN 810-005 WVR derived values (see later sections). A value of 13 mm/h rain rate was then estimated based on a fit to make the ITU model values match the DSN 810-005 values for Canberra, and thus, this value appears in Table 4 as another alternative rain rate for Canberra.

IV. Attenuation Statistics for Deep Space Network Sites

For deep-space link budgets, cumulative distributions of atmospheric attenuation for the DSN sites were obtained from multiyear data sets of WVR data and published in [1]. WVRs passively scan along the line of sight in the sky at different elevation angles measuring sky brightness temperature. Most of the time, the WVRs are pointed at zenith but periodically perform tipping curves at selected elevation angles for calibrations, or may be programmed to occasionally track a spacecraft such as for Cassini spacecraft radio science experiments. The DSN 810-005 model is based on actual water vapor radiometer brightness temperature measurements made at 31.4 GHz at all three DSN sites (Goldstone, Canberra, and Madrid). These models contain 143 months of Goldstone data (October 1993 through January 2009), 112 months of Canberra data (June 1999 through January 2009), and 189 months of Madrid data (September 1990 through January 2009) [1]. There were some cases of missing months of data from each site. In any event, these data sets are expected to accurately provide long-term statistics useful for link budgets and thus provide for reasonably accurate long-term models. For statistical characterization, all WVR measurements are converted to zenith values of brightness temperature. These measurements are filtered to remove erroneous points (such as when the Sun falls within its beam) and converted to atmospheric noise temperature contributions at 31.4 GHz.

Cumulative distributions at 31.4 GHz for each of the 12 months were calculated, then increased by a small amount (0.3 to 3 K, a function of frequency and noise temperature) to create a model for 32 GHz [1]. Year-average models for each site and frequency band were generated from the statistics extracted from the data. The model was also extrapolated to other frequency bands such as 2.3 GHz (S-band), 8.4 GHz (X-band), and 26 GHz (Ka-band) using known relationships.

The WVR-based measurements converted to atmospheric attenuation are expected to be more accurate than those obtained from ITU methods as they are based on multiple years of a data type that directly probes through the atmospheric path and includes effects due to both vapor and liquid water at the location of the tracking stations. It is also superior to other methods such as those using surface weather data as input to ITU models. Thus, attenuation statistics based on WVR measurements can be used to test the integrity of ITU models at sites where such data have been collected.

Thus, a cross-comparison of atmospheric attenuation calculated using three methods (ITU global maps/ITU models, weather data/ITU models, and WVR DSN 810-005) was performed for the three DSN sites at 8.4 GHz (X-band), 26 GHz (near-Earth Ka-band), and 32 GHz (deep-space Ka-band) frequencies.

V. Attenuation Comparisons (ITU versus DSN)

A. 8.4-GHz Attenuation Comparison for DSN Sites at 90-deg (Zenith) Elevation Angle

Table 5 presents total attenuation comparison results for Goldstone at 8.4 GHz (X-band) referenced to a 90-deg elevation angle (zenith) where the ITU model values include attenuation due to gas, rain, and clouds as calculated per Equation (11). The ITU rain rates provided in Table 4 were used in the calculation of the ITU rain attenuation. There is good agreement between the attenuation values derived from ITU global maps and values derived from ITU models using meteorological inputs derived from several years of weather data at each site. The ITU model and DSN 810-005 attenuation values include liquid contributions that increase with increasing CD values. There is reasonable agreement between the DSN 810-005 values and the ITU values with all differences lying at or below 0.015 dB. The comparison will take on a much different flavor when higher frequencies are considered (see later sections on 26 GHz and 32 GHz Ka-band).

Table 6 presents attenuation comparison results for Canberra at 8.4 GHz referenced to a 90-deg elevation angle (zenith) using ITU rain rate values (see Table 4). There is good agreement between the attenuation values derived from ITU global maps and those derived from ITU models using meteorological inputs derived from several recent years of weather data for the site. It is emphasized that the WVR values in the DSN 810-005 and ITU model values are sensitive to liquid contributions, which will be greater at higher CD values. There is better agreement between the DSN 810-005 values and the ITU values at the lower percentiles, with larger differences occurring at higher percentiles, such as a difference of 0.088 dB occurring at the 99th percentile (0.222 dB–0.134 dB). This implies a possible deficiency in the estimates based on liquid content. If we use an alternative value of rain rate (Table 4),

Table 5. Goldstone 8.4-GHz 90-deg elevation total attenuation (ITU rain rates).

Exceedence Percent	Availability Percent	ITU Global Maps Attn., dB	Weather Data/ ITU Model Attn., dB	DSN 810-005 Tables/Models Attn., dB
1.0	99.0	0.083	0.084	0.069
5.0	95.0	0.048	0.048	0.050
10.0	90.0	0.041	0.041	0.047
50.0	50.0	0.035	0.034	0.040

Table 6. Canberra 8.4-GHz 90-deg elevation total attenuation (ITU rain rates).

Exceedence Percent	Availability Percent	ITU Global Maps Attn., dB	Weather Data/ ITU Model Attn., dB	DSN 810-005 Tables/Models Attn., dB
1.0	99.0	0.220	0.222	0.134
5.0	95.0	0.106	0.107	0.069
10.0	90.0	0.076	0.078	0.058
50.0	50.0	0.046	0.046	0.046

these differences become somewhat smaller at all percentiles. The comparison will take on a much different flavor at higher frequencies (see later sections).

Table 7 presents results for Madrid at 8.4 GHz referenced to a 90-deg elevation angle (zenith). There is excellent agreement between the attenuation values derived from ITU models with global map inputs and values derived from ITU models using inputs derived from several years of local weather data. The ITU weather model attenuation values for Madrid are in reasonably good agreement with the DSN 810-005 attenuation values (up to ~0.02 dB difference at 99 percent weather). If we use an alternative value of rain rate based on DSN 810-005 rainfall (Slobin in Table 4), these differences become a somewhat larger, up to 0.076 dB at 99 percent CD. The comparison will take on a much different flavor at higher frequencies (see later sections).

Table 7. Madrid 8.4-GHz 90-deg elevation total attenuation (ITU rain rates).

Exceedence Percent	Availability Percent	ITU Global Maps Attn., dB	Weather Data/ ITU Model Attn., dB	DSN 810-005 Tables/Models Attn., dB
1.0	99.0	0.127	0.127	0.146
5.0	95.0	0.070	0.070	0.074
10.0	90.0	0.056	0.056	0.055
50.0	50.0	0.040	0.040	0.045

B. 8.4-GHz Attenuation Comparison for DSN Sites for 20-deg Elevation Angle

The attenuation estimates at 8.4 GHz for the DSN sites were also compared at a low elevation angle (20 deg) to examine whether there are any significant changes with ray path corrections. It is cautioned that at the lower elevation angle, scintillation may become signifi-

cant at high percentiles (as much as 0.07 dB at 99 percent weather). The scintillation fading combines with gas, cloud, and rain attenuation per Equation (10). However, for the purpose of this comparison, the scintillation fading was turned off since the WVR measurements are not sensitive to this contributor, and thus Equation (11) was used.

Table 8 presents results for Goldstone at 8.4 GHz (X-band) referenced to a 20-deg elevation angle. The ITU global map values and the ITU model values with weather data statistics input are again in good agreement. The ITU estimates are in good agreement, with the DSN 810-005 values at each percentile suggesting that the ITU models, at least at 8.4 GHz, are reasonably good at both elevation angles (20 deg in Table 8 and 90 deg in Table 5).

Table 8. Goldstone 8.4-GHz 20-deg elevation total attenuation (ITU rain rates).

Exceedence Percent	Availability Percent	ITU Global Maps Attn., dB	Weather Data/ ITU Model Attn., dB	DSN 810-005 Tables/Models Attn., dB
1.0	99.0	0.242	0.245	0.20
5.0	95.0	0.143	0.142	0.15
10.0	90.0	0.121	0.119	0.14
50.0	50..0	0.102	0.100	0.12

Table 9 presents results for Canberra at 8.4 GHz referenced to a 20-deg elevation angle. The ITU global map values and the ITU model values with weather data statistics input are again in good agreement. The ITU estimates are in good agreement with the DSN 810-005 values at the lowest percentiles, with the largest difference of 0.203 dB occurring at 99 percent, suggesting that the liquid contributions in the ITU estimates may be overestimated or too conservative. The Canberra results suggest that the ITU models at 8.4 GHz are reasonably good over a wide elevation angle range at 20 deg in Table 9 to 90 deg in Table 6.

Table 9. Canberra 8.4-GHz 20-deg elevation total attenuation (ITU rain rates).

Exceedence Percent	Availability Percent	ITU Global Maps Attn., dB	Weather Data/ ITU Model Attn., dB	DSN 810-005 Tables/Models Attn., dB
1.0	99.0	0.590	0.595	0.392
5.0	95.0	0.299	0.302	0.202
10.0	90.0	0.219	0.222	0.170
50.0	50.0	0.134	0.134	0.135

Table 10 presents results for Madrid at 8.4 GHz referenced to a 20-deg elevation angle. The ITU global map values and the ITU model values with weather data statistics input are in good agreement. The ITU model attenuation values exhibit reasonable agreement with the DSN 810-005 values at the lower CD values, with the biggest disagreement (0.364 dB versus 0.427 dB) occurring at the 99th percentile. The Madrid results suggest that the ITU gaseous model provides reasonable results as shown at 50 percent weather but the difference with the DSN WVR values becomes greater as the availability increases.

Table 10. Madrid 8.4-GHz 20-deg elevation total attenuation (ITU rain rates).

Exceedence Percent	Availability Percent	ITU Global Maps Attn., dB	Weather Data/ ITU Model Attn., dB	DSN 810-005 Tables/Models Attn., dB
1.0	99.0	0.362	0.364	0.427
5.0	95.0	0.206	0.206	0.216
10.0	90.0	0.164	0.164	0.161
50.0	50.0	0.119	0.118	0.132

C. 26-GHz Attenuation Comparison at 20-deg Elevation Angle

The comparison of atmospheric attenuation statistics at higher frequencies was also examined. Table 11 presents the results for Goldstone at 26 GHz referenced to a 20-deg elevation angle. The attenuation values predicted by ITU models far exceed the corresponding values from the DSN 810-005 document. The discrepancy is likely due to a combination of the ITU rain or cloud model being excessively pessimistic. Another reason may be that the models used in the translation of the raw WVR 31.4-GHz data to the 26-GHz attenuation values have higher errors due to 26 GHz being located closer to the 22-GHz water absorption line than at 8.4 GHz or 32 GHz.[5] Another reason for the larger discrepancies at 26 GHz could be due to the ITU global model values of rain rate and rain height used as input to ITU rain model have large uncertainties. To test this, the Slobin rain rate (derived from DSN 810-005 rainfall and as provided in Table 4) was input to the ITU rain model. The resulting ITU-derived attenuation values are in much better agreement with the DSN 810-005 attenuation values, as can be seen in Table 12.

Figure 2 displays the difference between the ITU model (with alternative rain rates from column four in Table 4) and DSN 810-005 attenuations at a 20-deg elevation angle for each of the three DSN sites as a function of CD value. The differences are smaller than ~0.4 dB at 50, 90, and 95 percentiles for all DSN sites. However, at 99 percent, the differences get as large as ~1.3 dB for Canberra, with the ITU model attenuation being consistently higher than the corresponding DSN 810-005 value for all DSN sites. The agreement is good for Goldstone and Madrid. It is suspected that the largest contribution to the discrepancies may be due to deficiencies in the rain model or its inputs. An alternative possibility is that the extrapolation from the WVR 31.4-GHz sky brightness temperature to the 26-GHz temperature (upon which attenuations are based) may not be optimal taking full effects of liquid into account. The discrepancies are much smaller at zenith, as can be discerned from Figure 3. The signatures in the attenuation differences at both elevation angles are similar (showing “hooks” near the 99th percentile), consistent with the higher uncertainties and variability of the rain rates, which are highly dependent on the microclimates and years over which the data were acquired.

D. 32-GHz Attenuation Comparison for DSN Sites for 90-deg (Zenith) Elevation Angle

A comparison of attenuation statistics between the ITU models and from the DSN at the deep-space Ka-band allocation at 32 GHz at zenith (90 deg) was also performed. Only the

[5] S. Slobin, personal communication, Jet Propulsion Laboratory, Pasadena, California, 2014.

Table 11. Goldstone 26-GHz 20-deg elevation total attenuation (ITU rain rates).

Exceedence Percent	Availability Percent	ITU Global Maps Attn., dB	Weather Data/ ITU Model Attn., dB	DSN 810-005 Tables/Models Attn., dB
1.0	99.0	2.947	3.022	1.822
5.0	95.0	1.413	1.389	0.830
10.0	90.0	1.060	1.003	0.716
50.0	50.0	0.617	0.547	0.439

Table 12. Goldstone 26-GHz 20-deg elevation total attenuation (5.75 mm/h rain rate).

Exceedence Percent	Availability Percent	Weather Data/ ITU Model Attn., dB	DSN 810-005 Tables/Models Attn., dB
1.0	99.0	2.098	1.822
5.0	95.0	1.096	0.830
10.0	90.0	0.834	0.716
50.0	50.0	0.506	0.439

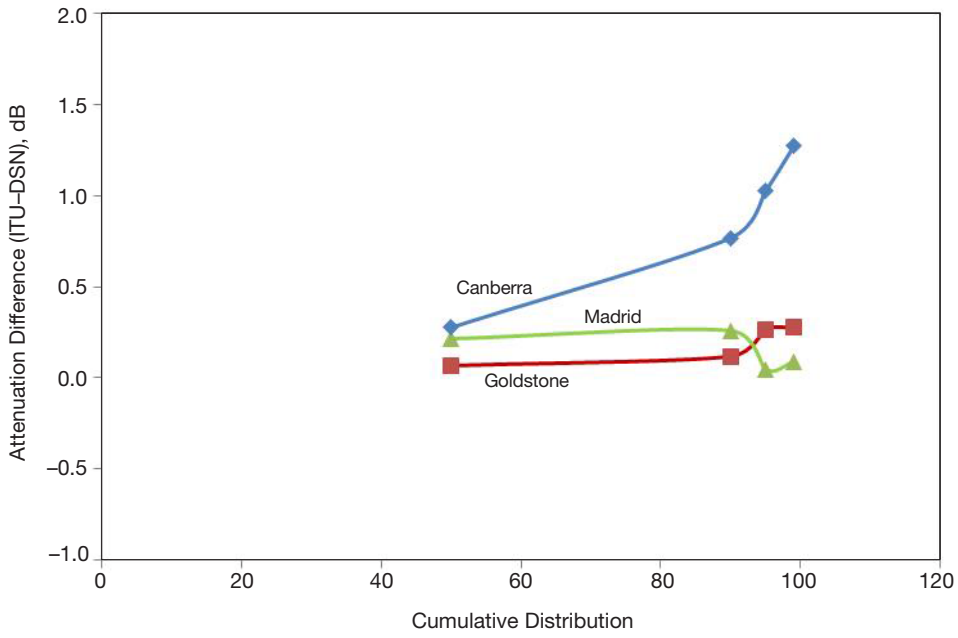

Figure 2. Difference of ITU (alternative rain rates) and DSN attenuation [1] versus CD at 26 GHz at a 20-deg elevation angle.

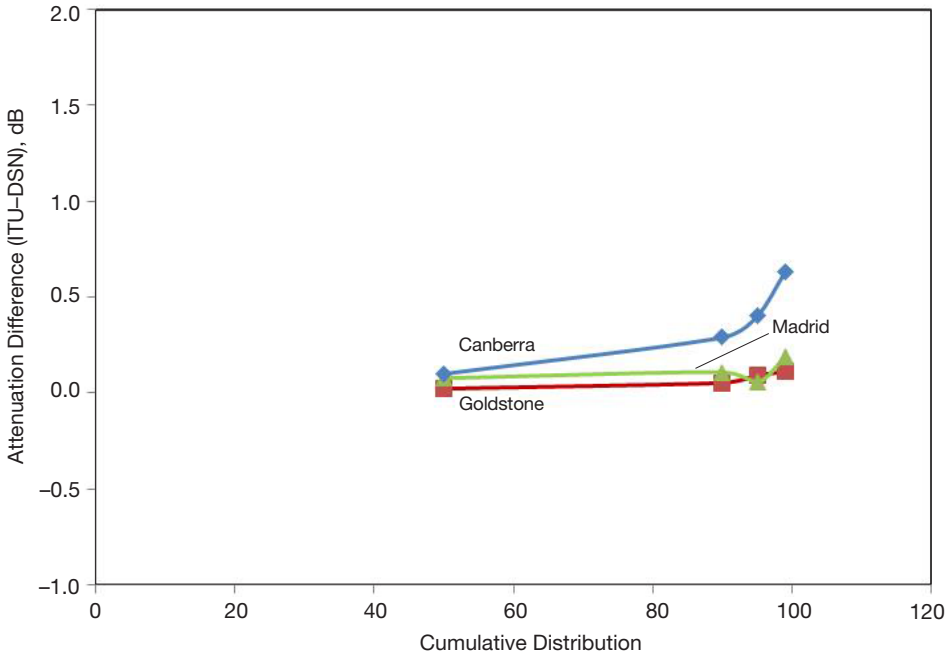

Figure 3. Difference of ITU (alternative rain rates) and DSN attenuation [1] versus CD at 26 GHz at zenith.

ITU model results using input gaseous parameters derived from Goldstone weather data are presented here, as there was little difference with the ITU model results using global map inputs. The baseline ITU rain attenuation estimates used rain rates and rain heights shown in Table 4 as inputs to the ITU rain models described in Section II. For 32 GHz, zenith scintillation fading is negligible but was not included as provided in Equation (11).

Table 13 presents a summary of the results for Goldstone at 32 GHz and at zenith. The ITU gaseous attenuation values always lie below the DSN 810-005 values. When adding the ITU rain and cloud attenuation to this, the ITU total attenuation values exceed the DSN 810-005 table values, the discrepancy becoming larger as the weather availability gets larger, suggesting that the ITU rain or cloud attenuation model is overly pessimistic as they have high uncertainties. Thus, at 50 percent weather, the DSN 810-005 yearly average of 0.167 dB is in better agreement with the ITU total of 0.194 dB than at 99 percent weather, where the DSN value of 0.586 dB lies significantly below the ITU value of 1.531 dB.

Using the alternative value of rain rate 5.75 mm/h given in Table 4, we get a much closer match of ITU total attenuation with the DSN 810-005 value, as can be seen in the last two columns of Table 14, except at the 99th percentile. If we remove cloud attenuation, the agreement becomes much better at all percentiles. The 5.75 mm/h rain rate is much lower than the ITU global map value of 18.818 mm/h, as it is derived from Goldstone rainfall statistics.[6] We assume that the ITU global map rain rate is subject to higher variation and higher uncertainty as it is referenced to a large global cell covering diverse terrains (coastal and desert) and there can be variation and nonuniformity with rain height, rain rate as well as other effects along the path.

[6] S. Slobin, personal communication, Jet Propulsion Laboratory, Pasadena, California, August 14, 2014.

Table 13. 32-GHz zenith attenuation estimate comparisons, Goldstone (rain rate = 18.818 mm/h).

CD, Percent	ITU Attn. (Gas), dB	ITU Attn. (Rain), dB	ITU Attn. (Cloud), dB	ITU Attn. (Total), dB	DSN 810-005 Attn., dB
50	0.155	0.040	0.000	0.194	0.167
90	0.205	0.168	0.013	0.387	0.260
95	0.230	0.298	0.058	0.587	0.304
99	0.305	0.994	0.232	1.531	0.586

Table 14. 32-GHz zenith attenuation estimate comparisons, Goldstone (rain rate = 5.75 mm/h).

CD, Percent	ITU Attn. (Gas), dB	ITU Attn. (Rain), dB	ITU Attn. (Cloud), dB	ITU Attn. (Total), dB	DSN 810-005 Attn., dB
50	0.155	0.010	0.000	0.164	0.167
90	0.205	0.044	0.013	0.262	0.260
95	0.230	0.080	0.058	0.369	0.304
99	0.305	0.287	0.232	0.825	0.586

Table 15 presents a summary of the 32-GHz zenith attenuation results for Madrid using the local weather data input to the ITU gaseous attenuation model and the ITU global map value of rain rate. Here we see that the ITU gaseous attenuation values for Madrid always lie below the DSN 810-005 values at each CD. When adding the ITU rain and cloud attenuation to this, the ITU total attenuation values exceed the DSN 810-005 table yearly average values for Madrid at all percentiles. If we use the alternative value of rain rate based on Madrid rainfall value provided in DSN 810-005 (see Table 4), we achieve better agreement of the ITU total attenuation with the DSN 810-005 values (see Table 16).

Table 17 presents a summary of the 32-GHz zenith attenuation results for Canberra using the local weather data input to the ITU gaseous attenuation model, the ITU global map values of rain rate for the rain model, and the standard ITU cloud attenuation model. Here we see that the ITU gaseous attenuation value for Canberra (Table 17) at 50 percent weather actually exceeds the DSN 810-005 value (but not by much), but the values at the higher percentiles lie below the DSN 810-005 values. When adding the ITU rain and cloud attenuation to this, the ITU total attenuation values significantly exceed the DSN 810-005 table yearly average values at all percentiles. If we use the Slobin rain rate parameter of 38.18 mm/h derived from DSN 810-005 rainfall and Crane curves [20] (see Table 4) to calculate rain attenuation, there is little change in the overall results relative to those obtained using the ITU global map value of 41.736 mm/h shown in Table 17. If we adjust the rain rate to a value of 13 mm/h to force the 99 percent ITU total attenuation (without cloud attenuation) to agree with that in DSN 810-005, then the ITU values lie much closer at 50 percent weather but are still significantly skewed at other percentiles, as shown in Table 18. If we remove cloud attenuation from the total for the ITU contribution, the agreement becomes much better, as expected from the fit of the rain rate parameter. Such effects are much more apparent in the 32-GHz results shown here than in the earlier discussion of results at 8.4 GHz. In any event, the fit (or adjustment) of the rain rate parameter to achieve agreement of the ITU total attenuation with the DSN total attenuation value at 99 percent is not strictly valid as it is not based on any actual rainfall data. A future task will involve estimating the rain rate from recent Canberra rain data to perform the comparison.

Table 15. 32-GHz zenith attenuation estimate comparisons, Madrid (rain rate = 29.1385 mm/h).

p, Percent	ITU, Gas	ITU, Rain	ITU, Cloud	ITU, Total	DSN 810-005 Yearly Avg.
50	0.206	0.077	0.000	0.283	0.217
90	0.262	0.316	0.099	0.677	0.361
95	0.279	0.555	0.206	1.036	0.636
99	0.317	1.773	0.438	2.528	1.670

Table 16. 32-GHz zenith attenuation estimate comparisons, Madrid (rain rate = 16.0655 mm/h).

p, Percent	ITU, Gas	ITU, Rain	ITU, Cloud	ITU, Total	DSN 810-005 Yearly Avg.
50	0.206	0.038	0.000	0.244	0.217
90	0.262	0.163	0.100	0.525	0.361
95	0.279	0.289	0.206	0.774	0.636
99	0.317	0.964	0.438	1.719	1.670

Table 17. 32-GHz zenith attenuation estimate comparisons, Canberra (rain rate = 41.736 mm/h).

p, Percent	ITU, Gas	ITU, Rain	ITU, Cloud	ITU, Total	DSN 810-005 Yearly Avg.
50	0.246	0.175	0.001	0.422	0.229
90	0.336	0.688	0.205	1.228	0.403
95	0.360	1.178	0.420	1.957	0.558
99	0.406	3.631	0.901	4.938	1.502

Table 18. 32-GHz zenith attenuation estimate comparisons, Canberra (rain rate = 13 mm/h).

p, Percent	ITU, Gas	ITU, Rain	ITU, Cloud	ITU, Total	DSN 810-005 Yearly Avg.
50	0.246	0.045	0.001	0.292	0.229
90	0.336	0.192	0.205	0.732	0.403
95	0.360	0.339	0.420	1.119	0.558
99	0.406	1.121	0.901	2.428	1.502

In summary, Goldstone attenuation derived from the ITU models using the alternative rain rate in Table 4 as input is in good agreement with the DSN 810-005 WVR-derived attenuation values for both zenith and 20-deg elevation angles. Canberra zenith attenuation values using the alternative (fitted) rain rate as input to the ITU model were in good agreement with the DSN 810-005 attenuation values when cloud attenuation is not considered. For Madrid, the agreement was good using the alternative rain rate in Table 4 for the input to the ITU rain model. However, at 20-deg elevation angle, the differences for Madrid were higher as much as 1.9 dB at 99 percent weather.

Using the alternative rain rates in Table 4 as input to the ITU models produced excellent to reasonable agreement at zenith with the WVR-derived values for all three sites. The excellent agreement using the lower alternative rain rate for Goldstone is consistent with the dry desert climate. However, the larger deviations seen for Madrid and Canberra, especially at 99 percent, may be indicative of several possible factors: rain rate and rain height may require modification, the combination of both the rain and cloud model may be "entangled" or overly conservative, or the models may break down at very high percentiles as other contributors may become significant for the wetter climate (scattering, rain decorrelation). The WVR data is also subject to higher uncertainties at the high percentiles due to significant amounts of liquid.

VI. White Sands and Svalbard ITU Model Attenuation Comparisons

Tables 19 and 20 display the attenuation referenced at zenith at 26 GHz estimated from the ITU global maps and from the ITU models using inputs derived from several years of recent weather data for White Sands, New Mexico and Svalbard, Norway, respectively. There is good agreement between the total attenuation values for the two ITU methods for all percentiles for White Sands (Table 19). This is due primarily to the similarity of the surface water vapor density statistics derived from both ITU global maps and from the surface weather data for White Sands (see Table 3). There is a somewhat larger discrepancy (but still small, ~0.03 dB) for Svalbard (Table 20) due to a somewhat higher difference in surface water vapor density for Svalbard (see Table 3). Note that both the rain and cloud attenuation values for both cases are the same, as no attempt was yet made to derive rain model inputs from recent rain gauge data. In any event, the inclusion of recent weather data to derive gaseous attenuation statistics did not result in any significant differences with those derived from ITU global maps for Svalbard and White Sands.

There are not yet any water vapor radiometer data or easily assessable signal attenuation data available to compare these ITU estimates against, as was the case with the DSN site comparisons. There is, however, an effort underway by NASA to statistically characterize the attenuation statistics at the Svalbard site, using a multichannel total power radiometer near 26 GHz along with the weather monitoring station (used in this study) to measure attenuation over a several-year period [6]. Such comparisons involving attenuation statistics extracted from radiometers at these sites are the focus of other studies.

Table 19. White Sands attenuation estimate comparison, 26 GHz, zenith.

CD, Percent	Global Maps/ITU Models				Weather Data/ITU Models			
	Gas, dB	Rain, dB	Cloud, dB	Total, dB	Gas, dB	Rain, dB	Cloud, dB	Total, dB
50	0.162	0.099	0.000	0.261	0.133	0.099	0.000	0.232
90	0.326	0.400	0.041	0.768	0.295	0.400	0.041	0.737
95	0.382	0.694	0.103	1.179	0.344	0.694	0.103	1.141
99	0.452	2.206	0.296	2.954	0.420	2.206	0.296	2.922
99.9	0.499	8.875	0.605	9.979	0.473	8.875	0.605	9.954

Table 20. Svalbard attenuation estimate comparison, 26 GHz, zenith.

CD, Percent	Global Maps/ITU Models				Weather Data/ITU Models			
	Gas, dB	Rain, dB	Cloud, dB	Total, dB	Gas, dB	Rain, dB	Cloud, dB	Total, dB
50	0.156	0.010	0.001	0.167	0.163	0.010	0.001	0.174
90	0.226	0.046	0.144	0.416	0.241	0.046	0.144	0.431
95	0.239	0.084	0.260	0.584	0.261	0.084	0.260	0.606
99	0.261	0.301	0.531	1.093	0.294	0.301	0.531	1.126
99.9	0.281	1.386	0.951	2.582	0.325	1.386	0.914	2.626

VII. ITU Scintillation Model Comparisons

A comparison on the magnitude of scintillation effects was performed using the wet refractivity from different sources as the principal input to ITU models as described in [15] for the DSN sites at Goldstone (Table 21), Canberra (Table 22), and Madrid (Table 23), and for the two NEN sites at White Sands (Table 24) and Svalbard (Table 25). Two cases were considered: one estimating scintillation fading from refractivity statistics derived from ITU global maps, and one estimating scintillation fading from refractivity statistics derived from several years of weather data (see Table 1). The scintillation fading model assumes 34-m-diameter antennas used in the aperture averaging correction term for the DSN antennas, and the largest diameter antenna at the two NEN sites (18 m for White Sands and 13 m for Svalbard). Tables 21–25 all assume an elevation angle of 10 deg. A frequency of 32 GHz is assumed for the DSN sites (Tables 21–23) and 26 GHz for the NEN sites (Tables 24–25). The "median" refractivity was then used as an input to estimating scintillation fading per the ITU models that also took into account elevation angle, link frequency, and antenna aperture. The results are very similar as the one major variable — the median refractivity input parameter to the models — did not change significantly between ITU maps and as derived from several years of recent weather data using ITU models (see Table 1). The magnitude of these results at the high CD values of 99 percent and 99.9 percent for Goldstone (~0.15 dB to 0.24 dB in Table 21) were consistent with scintillation fading measured during observations of the Cassini spacecraft at its Ka-band downlink frequency at 32 GHz at similar elevation angles using a 34-m-diameter antenna during similar wet weather conditions [21].

Table 21. Goldstone scintillation fading, dB.

CD, Percent	ITU Global Maps	ITU Model Weather Data
90	0.061	0.065
95	0.085	0.091
99	0.140	0.149
99.9	0.226	0.241

Table 22. Canberra scintillation fading, dB.

CD, Percent	ITU Global Maps	ITU Model Weather Data
90	0.081	0.085
95	0.114	0.119
99	0.188	0.195
99.9	0.303	0.316

Table 23. Madrid scintillation comparison.

CD, Percent	ITU Global Maps	ITU Model Weather Data
90	0.074	0.080
95	0.104	0.111
99	0.171	0.183
99.9	0.277	0.296

Table 24. White Sands scintillation fading comparison.

CD, Percent	ITU Global Maps	ITU Model Weather Data
90	0.177	0.167
95	0.248	0.234
99	0.409	0.386
99.9	0.660	0.622

Table 25. Svalbard scintillation fading comparison.

CD, Percent	ITU Global Maps	ITU Model Weather Data
90	0.189	0.206
95	0.264	0.288
99	0.435	0.476
99.9	0.702	0.768

VIII. Conclusions

This article provided details on a comparison performed on calculated atmospheric effects using different methods for the DSN and some NEN sites that are commonly used in telecommunications link budgets. Atmospheric attenuation estimated from ITU models was compared against atmospheric attenuation derived from WVR measurements at the three DSN sites and found to be in reasonable agreement, with some discrepancies believed to be consistent with higher uncertainties in the ITU models or their inputs, especially with the liquid content models (rain and clouds) at the higher percentiles. In previous years, this was not as important, as these estimates were conservative and NEN links operated at much higher margins. However, with the advent of higher data rates and lower margins in near-Earth communications links, it becomes more important to better characterize the performance of ITU models and identify any improvements that can be made. The DSN attenuation statistics provided a good testbed in which to cross-compare against the statistics of atmospheric losses derived from ITU data and models. In addition, atmospheric attenuation and scintillation fading using ITU models with different inputs were cross-compared and found to be in reasonable agreement.

Acknowledgments

I wish to thank James Nessel of NASA Glenn Research Center for providing the White Sands and Svalbard weather data used to derive some of the statistics discussed in this article, and Connie Dang of Exelis for assistance in providing multiyear DSN weather data sets. I wish to also thank Selahattin Kayalar of JPL for providing information on the ITU models used in this article as well as for providing very much appreciated comments. I also wish to thank Harvey Berger of Northrop Grumman Corporation for providing additional information on the ITU models and data used in this article as well as for his many appreciated comments and suggestions that resulted in significant improvement of the article. I also very much appreciate the reviews of early drafts of this article by Kar-Ming Cheung and Steve Slobin. I also wish to thank Bruce MacNeal and David Heckman for providing computational assistance.

References

[1] S. D. Slobin, "Atmospheric and Environmental Effects," *DSN Telecommunications Link Design Handbook*, DSN No. 810-005, Space Link Interfaces, Module 105, Rev. D, Jet Propulsion Laboratory, Pasadena, California, September 15, 2009. http://deepspace.jpl.nasa.gov/dsndocs/810-005/105/105D.pdf

[2] International Telecommunication Union, "The Radio Refractivity Index: Its Formula and Refractivity Data," Recommendation ITU-R P.453-10, Electronic Publication, Geneva, Switzerland, February 2012.

[3] International Telecommunication Union, "Method for Calculating Link Performance in the Space Research Service," Recommendation ITU-R SA.2183, Electronic Publication, Geneva, Switzerland, October 2010.

[4] International Telecommunication Union, "Water Vapour: Surface Density and Total Columnar Content," Recommendation ITU-R P.836-3, Electronic Publication, Geneva, Switzerland, November 2001.

[5] R. Acosta, M. Zemba, J. Morse, and J. Nessel, "Two Years of Simultaneous Ka-Band Measurements: Goldstone, Ca.; White Sands, NM; and Guam, USA," Proceedings of the 18th Ka and Broadband Communications Conference, Ottawa, Canada, September 24–27, 2012.

[6] R. Acosta, J. Morse, J. Nessel, M. Zemba, K. Tuttle, A. Caroglanian, B. Younes, and Sten-Chirstian Pedersen, "Ka-Band Site Characterization of the NASA Near Earth Network in Svalbard, Norway," Proceedings of the 17th Ka and Broadband Conference, Palermo, Italy, October 3–5, 2011.

[7] R. Crane, *Electromagnetic Wave Propagation through Rain*, John Wiley and Sons, 1996.

[8] International Telecommunication Union, "Specific Attenuation Model for Rain for Use in Prediction Methods," Recommendation ITU-R P.838-3, Electronic Publication, Geneva, Switzerland, March 2005.

[9] International Telecommunication Union, "Characteristics of Precipitation for Propagation Modeling," Recommendation ITU-R P.837-5, Electronic Publication, Geneva, Switzerland, 2007.

[10] G. Blarzino, N. Jeannin, L. Castanet, D. Ferraro, L. Luini, C. Capsoni, and A. Martellucci, "Discussion Document about Recommendation ITU-R P.837-4," Input Document 3J/185-3M/217, April 11, 2007.

[11] L. Castanet, G. Blarzino, N. Jeannin, A. Testoni, C. Capsoni, et al., "Assessment of Radiowave Propagation for Satellite Communication and Navigation Systems in Tropical and Equatorial Areas," Final Report, ESA Study n° ESTEC 18278/04/NL/US, Report ONERA RF 4/09521 DEMR, June 2007.

[12] International Telecommunication Union, "Rain Height Model for Prediction Methods," Recommendation ITU-R P.839-4, Electronic Publication, Geneva, Switzerland, November 2013.

[13] International Telecommunication Union, "Attenuation by Atmospheric Gases," Recommendation ITU-R P.676-9, Electronic Publication, Geneva, Switzerland, February 2012.

[14] International Telecommunication Union, "Annual Mean Surface Temperature," Recommendation ITU-R P.1510, Electronic Publication, Geneva, Switzerland, February 2001.

[15] International Telecommunication Union, "Propagation Data and Prediction Methods Required for the Design of Earth–Space Telecommunications Systems," Recommendation ITU-R P.618-11, Electronic Publication, Geneva, Switzerland, September 2013.

[16] C. H. Lee, K.-M. Cheung, and C. Ho, "A Unified Low-Elevation-Angle Scintillation Model," *The Interplanetary Network Progress Report*, vol. 42-185, Jet Propulsion Laboratory, Pasadena, California, pp. 1–13, May 15, 2011.
http://ipnpr.jpl.nasa.gov/progress_report/42-185/185A.pdf

[17] International Telecommunication Union, "Reference Standard Atmospheres," Recommendation ITU-R P.835-5, Electronic Publication, Geneva, Switzerland, February 2012.

[18] International Telecommunication Union, "Effects of Tropospheric Refraction on Radiowave Propagation," Recommendation ITU-R P.834-6, Electronic Publication, Geneva, Switzerland, January 2007.

[19] International Telecommunication Union, "Probability Distributions Relevant to Radiowave Propagation Modeling," Recommendation ITU-R P.1057-3, Electronic Publication, Geneva, Switzerland, September 2013.

[20] R. Crane, "Prediction of Attenuation by Rain," *IEEE Transactions on Communications*, vol. COM-28, no. 9, pp. 1717–1733, September 1980.

[21] D. D. Morabito, "Detection of Tropospheric Propagation Effects from Deep Space Links of the Cassini Spacecraft," *Radio Science*, vol. 42, no. 6, RS6007, December 2007. doi:10.1029/2007RS003642
http://onlinelibrary.wiley.com/doi/10.1029/2007RS003642/abstract

[22] International Telecommunication Union, "Attenuation due to Clouds and Fog," Recommendation ITU-R P.840-6, Electronic Publication, Geneva, Switzerland, September 2013.

[23] International Telecommunication Union, "Guide to the Application of the Propagation Methods of Radiocommunication Study Group 3," Recommendation ITU-R P.1144-6, Electronic Publication, Geneva, Switzerland, February 2012.